Available online at www.sciencedirect.com
SCIENCE DIRECT®
International Journal of Mass Spectrometry 234 (2004) 123–130
International Journal of Mass Spectrometry
www.elsevier.com/locate/ijms

Rapid electron capture dissociation of mass-selectively accumulated oligodeoxynucleotide dications

Kristin N. Schultz, Kristina Håkansson*

Department of Chemistry, University of Michigan, 930 North University Avenue, Ann Arbor, MI 48109-1055, USA

Received 7 January 2004; accepted 4 February 2004

Dedicated to Professor Alan G. Marshall on the occasion of his 60th birthday.

Available online 14 April 2004

Abstract

We have performed extended characterization of the fragmentation patterns of oligodeoxynucleotide dications following electron capture dissociation (ECD) utilizing improved instrumentation. Our current results from a 9.4 T Fourier transform ion cyclotron resonance mass spectrometer equipped with mass-selective external ion accumulation and an indirectly heated dispenser cathode electron source demonstrate much richer fragmentation than from a previous 7 T instrument with a directly heated filament electron source. We propose the previous absence of backbone product ions from purine-containing oligonucleotides is a result of intramolecular hydrogen bonding, preventing product ions from separating. Similar behavior is observed at non-optimized ECD conditions with the current instrumentation. However, infrared laser heating of the resulting charge-reduced radical species results in extensive backbone fragmentation (different from infrared multiphoton dissociation) of the oligonucleotide dA_6, demonstrating potential for ECD to characterize nucleic acid secondary structure. Under more optimized conditions, rich fragmentation, mostly in terms of w, (a/z − B), and (c/x − B) products, is observed for dA_6, dC_6, dG_5, and d(GCATGC) following ECD only, allowing complete sequencing in several cases. The current ECD spectra contain some doubly charged products, indicating that populations of gas-phase oligodeoxynucleotide dications are zwitterionic.

Keywords: ECD; Electron capture dissociation; Fourier transform ion cyclotron resonance; ICR; FT-ICR; Mass spectrometry; FTMS; Electrospray; ESI; Oligonucleotide; DNA

1. Introduction

Most tandem mass spectrometry (MS/MS) strategies for determining oligonucleotide primary structure are based on the dissociation of even-electron anions [1–3]. For example, both collision activated dissociation (CAD) [4–6] and infrared multiphoton dissociation (IRMPD) [7–9] of electrosprayed oligonucleotides provide backbone fragmentation, mainly in terms of w and (a − B) ions, in which B corresponds to the nucleobase closest to the cleavage site [4], see Scheme 1. Matrix-assisted laser desorption/ionization (MALDI) post-source decay of oligonucleotide anions resulted in a more diverse fragmentation pattern, including x/b, y/c, and z/d products in similar abundance as the $w/(a-B)$ ion pairs [10]. Fragmentation of oligonucleotide cations formed by electrospray ionization (ESI) [11–14], or MALDI [15], has also been investigated by several research groups. A disadvantage, in both the positive and negative ion cases, is that a major dissociation channel corresponds to nucleobase loss only, which does not provide sequence information. Also, secondary fragmentation, including water and additional base loss, complicate spectral interpretation and reduce sensitivity. Enhanced sensitivity has been reported by Hannis and Muddiman through incorporation of a 7-deaza purine analog, eliminating the extensive depurination fragmentation channel [16].

CAD of radical gas-phase oligonucleotide anions was demonstrated by McLuckey et al. through ion–ion reactions, resulting in additional and complementary sequence information compared to CAD of even-electron ions [17]. Recently, Hvelplund and coworkers reported similar results from high-energy collisions between oligonucleotide anions and noble gases [18]. Electron capture dissociation

* Corresponding author. Tel.: +1-734-615-0570; fax: +1-734-647-4865.
E-mail address: kicki@umich.edu (K. Håkansson).

1387-3806/$ – see front matter © 2004 Elsevier B.V. All rights reserved.
doi:10.1016/j.ijms.2004.02.019

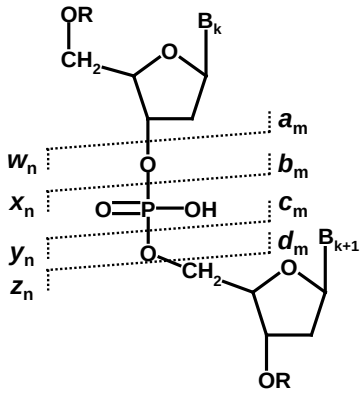

Scheme 1. Nomenclature for oligonucleotide backbone product ions, adapted from reference [4]. Products containing the 5′ end of the oligonucleotide are termed *a*, *b*, *c*, and *d* ions, whereas products containing the 3′ end are termed *w*, *x*, *y*, and *z* ions, respectively. The subscript, *n* or *m*, indicates the number of nucleotide residues present in that particular fragment.

(ECD), which involves radical ion formation, has proven to provide unique fragmentation patterns for multiply charged peptide and protein [19–21], polymer [22,23], peptide nucleic acid [24], and lantibiotic [25] cations. Håkansson et al. recently explored the utility of ECD for sequencing oligonucleotide dications utilizing an ECD implementation based on a directly heated filament [26]. Only limited fragmentation occurred, but the dissociation channels differed from IRMPD of the same species. Here, we present extended work, including novel fragmentation pathways and increased sequence coverage, for larger precursor ion populations (made possible through mass-selective external ion accumulation) [27,28] and by use of an indirectly heated dispenser cathode electron source [29–31], allowing rapid (∼50 ms versus 30 s) ECD.

2. Experimental

2.1. Sample preparation

The oligodeoxynucleotides dC_6, dG_5, dA_6, and d(GCATGC) were purchased as their crude ammonium salts from Tri-Link BioTechnnologies (San Diego, CA) and used without further purification. The lyophilized samples were dissolved in HPLC grade water (J.T. Baker, Philipsburg, NJ) to a concentration of ∼1 mM. Prior to electrospray ionization, the stock solutions were diluted 10-fold into 1:1 water/methanol (Baker) containing 0.5% formic acid (Sigma Chemical Co., St. Louis, MO).

2.2. ECD MS/MS

All experiments were performed with a passively shielded 9.4 T quadrupole-Fourier transform ion cyclotron resonance (Q-FT-ICR) mass spectrometer [32] located in the laboratory of Professor Alan G. Marshall at the National High Magnetic Field Laboratory in Tallahassee, FL. The acidic oligonucleotide solutions were infused through a tapered microelectrospray [33] emitter (50 μm i.d.) at a flow rate of 300 nl/min. Ions were preaccumulated in a first octopole for 100 ms, transferred through a quadrupole mass filter operating in mass-selective mode at the mass-to-charge (*m*/*z*) ratio of interest, and stored in a second octopole, kept at an elevated pressure (∼10^{-3} Torr) and modified to allow improved ion ejection along the *z*-axis [34]. The experimental event sequence "accumulation, mass selection/accumulation" was looped 25–600 times to build-up a precursor ion signal-to-noise (S/N) ratio of ∼1000:1. Mass-selectively accumulated ions were transferred through an octopole ion guide and captured by gated trapping in an open cylindrical cell [35]. Stored-waveform inverse Fourier transform (SWIFT) [36,37] ejection was applied to further isolate the oligonucleotide ion under investigation. ECD was performed by pulsing a grid located in front of the electron source (a 10-mm diameter dispenser cathode, HeatWave, Watsonville, CA) to +150 V for 80 ms. During the ECD event, the bias voltage of the cathode was −0.2 V and the trapping plates of the cell were kept at 5 V. Immediately following the ECD event, the trap plates were set to 2 V, the grid to 5 V, and the cathode bias to 10 V for 10 ms to collect remaining electrons. The cathode heating power was 11 W. Following ECD, product ions were subjected to chirp excitation (72–720 kHz at 150 Hz/μs) and direct-mode broadband detection (512 Kword data points). A Hanning window function was applied and the data set was zero filled once prior to fast Fourier transform followed my magnitude calculation. Internal frequency-to-*m*/*z* conversion was performed with a two-term calibration equation [38,39] based on the measured frequencies of the $[M + 2H]^{2+}$ and $[M + 2H]^{+\bullet}$ or $[M + H]^{+}$ ions of the investigated oligonucleotides. The experimental event sequence was controlled by a MIDAS data acquisition system [40]. Displayed spectra represent a sum of 5–30 time-domain transients.

2.3. ECD MS/MS and ECD/IRMPD MS^3 of dA_6

The oligonucleotide dA_6 was also subjected to ECD under different conditions than described above. In that experiment, the electron irradiation time was 20 ms, the bias voltage of the cathode was −5 V, and the grid voltage was +5 V. The resulting charge-reduced species (see below) was SWIFT isolated and irradiated with infrared photons (10.6 μm) from an off-axis [31] 40 W CO_2 laser for 250 ms at 15% laser power.

3. Results and discussion

3.1. Initial ECD MS/MS and ECD/IRMPD MS^3 of dA_6

In our previously published experiments [26], doubly protonated dA_6 and dG_7 showed different behavior following electron irradiation compared to the other oligodeoxynu-

cleotides studied (dC_4–dC_7, dG_5, and d(GCATGC)): in the two former cases an abundant charge-reduced species was detected along with one minor product, corresponding to the loss of one nucleobase, whereas, the other oligodeoxynucleotides displayed various degrees of backbone cleavage. The dA_6/dG_7 behavior can be related to gas-phase intramolecular hydrogen bonding, preventing product ions from separating (and, thus, being detected) in a manner analogous to what has been observed for proteins [41–43]. The introduction of activated ion ECD [41] demonstrated that ion preheating to disrupt non-covalent interactions responsible for higher order structure results in detection of a much larger variety of product ions following ECD of proteins. Molecular modeling demonstrated gas-phase intramolecular hydrogen bonding in protonated purine monophosphates [44]. Also, gas-phase hydrogen/deuterium exchange of positively charged mononucleotides showed that deoxyadenosine monophosphate exchanged much slower than other deoxynucleoside monophosphates [45], further confirming the presence of intramolecular hydrogen bonds because affected hydrogens would likely be inaccessible to exchange.

Encouraged by the literature discussed above, we utilized a 9.4 T FT-ICR instrument to perform an MS^3 experiment in which the charged reduced radical species from electron irradiation of dA_6 was SWIFT isolated and irradiated with infrared photons, similar to what has been previously shown for glyco- [31] and phosphopeptides [46]. The resulting spectrum is shown in Fig. 1 (bottom). The spectrum resulting from ECD only is shown in the same figure (top). As in our previous experiments on a 7 T instrument equipped with a heated filament electron source [26], the major product

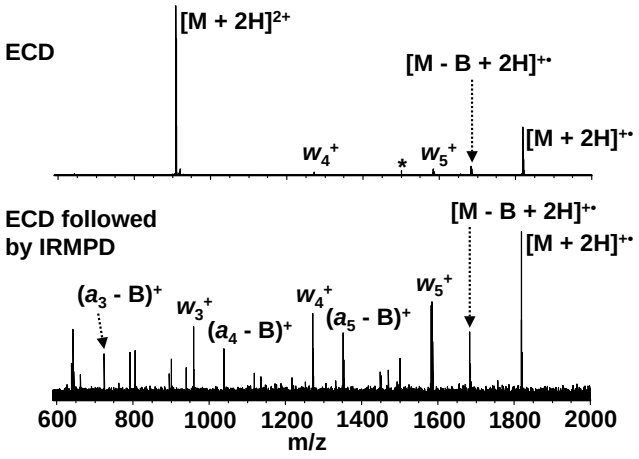

Fig. 1. ECD MS/MS (top) and ECD/IRMPD MS^3 (bottom) of dA_6 at an electron irradiation time of 20 ms, a cathode bias voltage of −5 V and a grid extraction voltage of +5 V (30 scans). The laser irradiation time in the MS^3 experiment was 250 ms at 6 W laser power. Solely a charge-reduced radical species and two very minor backbone products are observed following ECD. IR laser heating of the charge-reduced radical results in several backbone fragments, corresponding to cleavage in between all nucleotides. Peaks labeled as *w* ions can also be *d* ions, and peaks labeled as *a* ions can be *z* ions because of the symmetrical nature of dA_6.

following electron irradiation is the charge-reduced radical species. Only minor (∼5% relative abundance) hydrogen atom ejection to form an even-electron singly charged species is observed. Contrary to the previous experiments, two products corresponding to backbone cleavage (w_4/d_4 and w_5/d_5) are observed following ECD on the 9.4 T instrument (because of the symmetrical nature of dA_6, *w*, and *d* ions cannot be distinguished by mass alone). We believe the detection of two backbone products can be attributed to the improved instrumentation utilized for the current experiments: because ECD is a rather inefficient process in terms of precursor-to-product ion conversion (particularly for the low charge states investigated here—the electron capture cross section increases with the square of the ion charge) [19–21], the S/N ratio of the precursor ion prior to ECD is crucial. Mass-selective external ion accumulation [27,28] (not available on the previous 7 T instrument) allows precursor ion build-up without sacrificing spectral quality due to space–charge effects resulting from the presence of contaminant species (which are always present following oligonucleotide synthesis). Also, the trapped ion cell of the utilized 9.4 T instrument is larger in volume than for the previously used 7 T instrument, allowing a larger ion population to be stored without interference from space–charge effects. A concurrent positive effect may also result from the increased magnetic field strength (the maximum number of trapped ions increases quadratically with increasing field strength) [47]. Finally, the utilized 9.4 T instrument is equipped with an indirectly heated dispenser cathode electron source [29–31], providing a larger flux of collimated electrons than a directly heated filament.

The w_4/d_4 and w_5/d_5 backbone products also result from thermal dissociation (via laser activation) of the charge-reduced radical species (Fig. 1 bottom). However, in that MS^3 experiment, one additional *w*/*d* ion is observed along with three complementary (a/z − B) ions (see Scheme 1). These product ions correspond to cleavage in between all nucleotide residues in dA_6. Detection of (a/z − B) ions was not expected because such an ion was only observed in one case (from dC_4) in the previous experiments. However, (w/d − B) ions were seen in many cases [26]. Care was taken to ensure that the (a/z − B) ions are not a result of IRMPD only: no dissociation of the doubly charged precursor ion was observed at the laser fluence used. Also, the IRMPD spectra of doubly protonated dA_6 obtained at higher laser fluence significantly differ in appearance compared to the MS^3 spectrum in Fig. 1 (bottom) (data not shown). The detection of a much larger variety of product ions following laser heating of the charge-reduced radical species strongly supports the presence of gas-phase intramolecular hydrogen bonds, preventing the products from separating following ECD only.

3.2. Improved ECD of dA_6

The ECD conditions used to obtain the spectra presented in Fig. 1 had been found to work well for peptides and were,

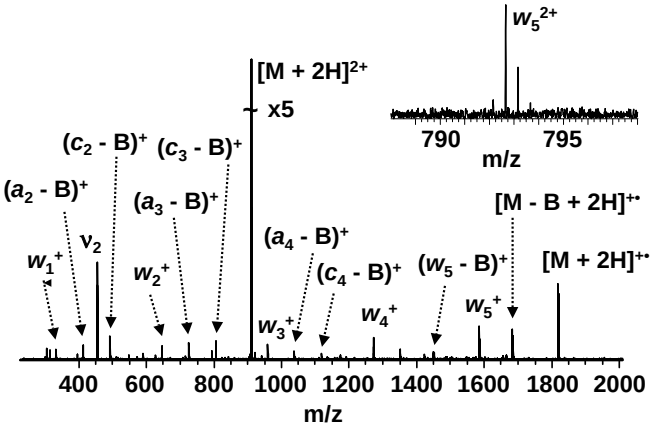

Fig. 2. ECD (20 scans) of dA_6 at different conditions than in Fig. 1. Here, the irradiation time was 80 ms, the cathode bias voltage was −0.2 V and the grid extraction voltage was +150 V. Rich fragmentation is observed, including a complete *w*/*d* ion series (only the *w* label is given), and several (*a*/*z* − B) and (*c*/*x* − B) ions (only the *a* and *c* labels are given). The inset shows one out of three doubly charged product ions (see Table 1). Such ions are typically not observed from ECD of doubly charged precursor ions because electron capture reduces the total charge by one. However, detection of such product ions is possible if the precursor ion is zwitterionic.

therefore, also employed in our initial oligonucleotide experiments. However, upon varying the ECD conditions, it was found that the spectral appearance can change drastically. Fig. 2 shows ECD of dA_6 under a different set of conditions as compared to Fig. 1 (top). Here, the electron irradiation time was longer (80 ms versus 20 ms), the cathode bias voltage was changed from −5 to −0.2 V, and the grid extraction voltage was +150 V instead of +5 V. The resulting ECD spectrum contains a plethora of different product ions, including a complete *w*/*d* ion series and several (*a*/*z* − B) and (*c*/*x* − B) ions. The three product ions detected at the earlier conditions (Fig. 1, top) are still the most abundant products. For a complete list of assigned product ions, see Table 1. The improvement in information content can be attributed to the longer electron irradiation time, which may allow more product ions to be formed. Also, the lower cathode bias voltage should provide more electrons at the low energy required for ECD to take place. Finally, the much higher grid extraction voltage should result in more efficient electron injection into the ICR cell.

From Table 1 it is seen that in addition to the ions mentioned above, *a*/*z* and *c*/*x* ions that retained all nucleobases are observed (i.e. only one bond is cleaved). The S/N ratios of those ions are too low for them to be visible on the scale of Fig. 2. In our earlier experiments such *a*/*z* ions were also seen. However, in that case they were detected as radical ions [26]. More interestingly, Table 1 includes three doubly charged product ions, which are not expected from ECD of a doubly charged species (electron capture reduces the total charge by one and, thus, all product ions should be singly charged or neutrals). The inset in Fig. 2 shows one of those doubly charged products, identified as $w_5/d_5{}^{2+}$. The same

Table 1
Product ions observed following ECD (80 ms irradiation, −0.2 V bias, +150 V grid) of dA_6

Observed *m*/*z*	Calculated *m*/*z*	Assignment	Error (ppm)
332.0757	332.0755	$w_1/d_1{}^+$	0.6
492.0687	492.0679	$(c_2/x_2 - B)^+$	1.6
645.1339	645.1331	$w_2/d_2{}^+$	1.2
716.1263	716.1246	$(c_5/x_5 - B)^{2+}$	2.4
725.1601	725.1592	$(a_3/z_3 - B)^+$	1.2
792.6585	792.6566	$w_5/d_5{}^{2+}$	2.4
805.1275	805.1255	$(c_3/x_3 - B)^+$	2.5
841.6759	841.6755	$[M - B + 2H]^{2+}$	0.5
860.2155	860.2139	$a_3/z_3{}^+$	1.9
909.2022	909.2022	$[M + 2H]^{2+}$	Calibrant
940.1811	940.1800	$c_3/x_3{}^+$	1.2
958.1929	958.1908	$w_3/d_3{}^+$	2.2
1038.2171	1038.2169	$(a_4/z_4 - B)^+$	0.2
1118.186	1118.183	$(c_4/x_4 - B)^+$	2.7
1136.195	1136.194	$(w_4/d_4 - B)^+$	0.9
1173.2714	1173.2715	$a_4/z_4{}^+$	−0.09
1191.283	1191.282	$b_4/y_4{}^+$	0.8
1271.250	1271.248	$w_4/d_4{}^+$	1.6
1351.221	1351.275	$(a_5/z_5 - B)^+$??	−40
1431.246	1431.241	$(c_5/x_5 - B)^+$	3.5
1449.254	1449.252	$(w_5/d_5 - B)^+$	1.4
1486.320	1486.330	$a_5/z_5{}^+$	−6.7
1548.293	1548.298	$[M - 2B + 2H]^{+\bullet}$	−3.2
1567.302	1567.303	$c_5/x_5{}^+$	−0.6
1584.302	1584.306	$w_5/d_5{}^+$	−2.5
1602.319	1602.317	$(w_5/d_5 + H_2O)^+$	1.2
1665.343	1665.341	$[M - B - H_2O + 2H]^{+\bullet}$	1.2
1683.3508	1683.3510	$[M - B + 2H]^{+\bullet}$	−0.1
1817.399	1817.397	$[M + H]^+$	1.1
1818.4050	1818.4050	$[M + 2H]^{+\bullet}$	Calibrant

fragment is also present in singly charged form. Zubarev and coworkers have demonstrated detection of singly charged product ions from singly charged species via interaction of the precursor ion with higher energy (∼20 eV) electrons than in ECD. That process was termed electronic excitation dissociation (EED), which can be utilized to investigate electron interaction reactions of ions produced by MALDI [48]. Because we were using very low energy (∼0.2 eV) electrons in the current experiments, we did not believe the detection of doubly charged products could be attributed to an EED-type process. However, EED has only been demonstrated for peptide ions and the effect for oligonucleotide ions is unknown. Thus, we varied the electron energy (see Fig. 3) but the abundance of the $w_5/d_5{}^{2+}$ ion did not change drastically. Also, several experiments were performed to ensure the $w_5/d_5{}^{2+}$ ion was not present prior to electron irradiation. Zubarev has suggested an alternative explanation [49]: if the precursor is zwitterionic, doubly charged products can be formed from a precursor with a net charge of 2. For the oligonucleotides studied here, zwitterion formation is likely because most backbone phosphate groups are deprotonated in solution at the current pH (∼2). Protonation of more than two nucleobases with concurrent deprotonation of one or more backbone phosphate groups will yield a gas-phase

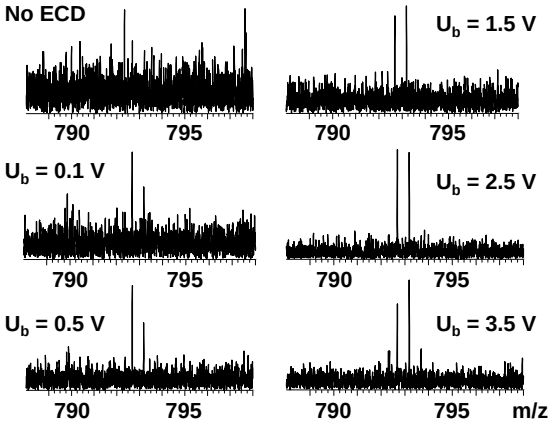

Fig. 3. Abundance of the doubly charged w_5/d_5 product (see Fig. 2) following ECD (5 scans) of doubly charged dA_6 at various cathode bias voltages (U_b). The w_5/d_5^{2+} ion is not detected when electron irradiation is absent. Also, its magnitude does not change drastically with increasing cathode bias voltage, excluding an electronic excitation process to be the cause of its formation. Thus, we conclude that a population of dA_6 dications is zwitterionic, allowing formation of doubly charged products from a doubly charged precursor.

zwitterion with a net charge of two. The detection of both w_5/d_5^{2+} and $(c_5/x_5 - B)^{2+}$ suggests at least two different dA_6 zwitterions are present. Finally, a very minor product ion was identified as $(w_5/d_5 + H_2O)$. Such ions were previously detected from dC_5–dC_7 and speculations on their formation were presented in that article [26].

3.3. Improved ECD of dC_6

Encouraged by the improved ECD for dA_6, we proceeded to investigate the dissociation patterns of a few other small oligonucleotides at the ECD conditions presented above, starting with dC_6. The resulting ECD spectrum is shown in Fig. 4 and the assigned product ions are listed in Table 2. As

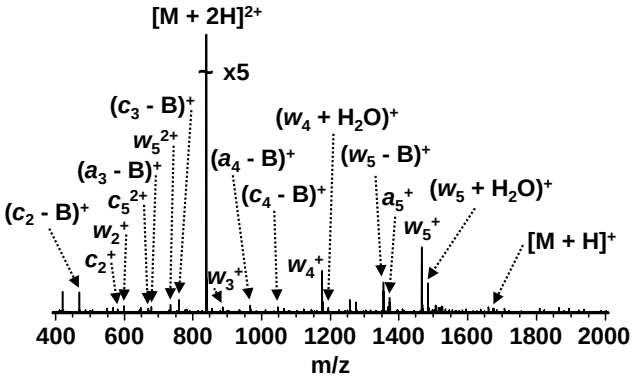

Fig. 4. ECD (20 scans) of dC_6 at the improved ECD conditions found for dA_6 (see Fig. 2). Again, a much larger variety of product ions is observed compared to earlier experiments, mostly in terms of w/d, $(a/z - B)$ and $(c/z - B)$ ions (only the former labels are given). In addition, a/z and c/x ions that retained all nucleobases are detected. As for dA_6, zwitterionic precursor ions are indicated by the presence of doubly charged products.

Table 2
Product ions observed following ECD (80 ms irradiation, −0.2 V bias, +150 V grid) of dC_6

Observed m/z	Calculated m/z	Assignment	Error (ppm)
468.0573	468.0568	$(c_2/x_2 - B)^+$	1.1
579.1005	579.1000	c_2/x_2^+	0.9
597.1111	597.1107	w_2/d_2^+	0.5
668.1025	668.1016	$(c_5/x_5 - B)^{2+}$	1.3
677.1376	677.1368	$(a_3/z_3 - B)^+$	1.2
732.6289	732.6335	w_5/d_5^{2+}	−6.3
757.1038	757.1031	$(c_3/x_3 - B)^+$	0.9
781.6480	781.6475	$[M - B + 2H]^{2+}$	0.6
837.1685	837.1685	$[M + 2H]^{2+}$	Calibrant
855.1390	855.1400	$(a_4/z_4 - 2B)^+$	−1.2
886.1578	886.1571	w_3/d_3^+	0.8
966.1845	966.1832	$(a_4/z_4 - B)^+$	1.3
1046.1502	1046.1500	$(c_4/x_4 - B)^+$	0.2
1064.161	1064.160	$(w_4/d_4 - B)^+$	0.7
1076.221	1076.218	$(a_4/z_4 - H^\bullet)^+$	2.8
1175.2033	1175.2034	w_4/d_4^+	−0.09
1193.213	1193.214	$(w_4/d_4 + H_2O)^+$	0.8
1242.165	1242.173	$(w_5/d_5 - 2B)^+$	−6.4
1335.195	1335.196	$(c_5/x_5 - B)^+$	−0.7
1353.2067	1353.2065	$(w_5/d_5 - B)^+$	0.1
1366.267	1366.273	a_5/z_5^+	−4.4
1464.249	1464.260	w_5/d_5^+	−7.5
1482.260	1482.270	$(w_5/d_5 + H_2O)^+$	−6.7
1564.298	1564.302	$[M - B + H^\bullet]^+$	−2.7
1673.3298	1673.3298	$[M + H]^+$	Calibrant

for dA_6, abundant w/d, $(a/z - B)$, and $(c/x - B)$ ions are observed along with minor a/z and c/x products. That result is in stark contrast to our previous experiments in which only two consecutive w/d ions (w_4/d_4 and w_5/d_5) and one radical a/z ion ($a_5/z_5H^\bullet$) were detected [26]. Those three products (a_5/z_5 as an even-electron ion) are also the most abundant in the current experiments along with $(c_2/x_2 - B)$, which was not observed in the previous experiments. The current product ions correspond to cleavage in between all nucleotide residues. Similar to dA_6, three doubly charged product ions are seen, indicating at least two different dC_6 zwitterions are present. Finally, abundant products corresponding to w_4/d_4 and w_5/d_5 plus water are seen, as was the case in the previous experiments.

3.4. Improved ECD of dG_5

The product ion spectrum following ECD of mass-selectively accumulated dG_5 dications is shown in Fig. 5 and product ion assignments are given in Table 3. In the previous experiments, dG_5 showed a different behavior than the other oligonucleotides in that the dominant product ions were radical ions and that facile nucleobase and water loss was observed [26]. Facile guanine base loss was also seen in ECD of PNAs [24]. Again, product ions resulting from the previously observed fragmentation channels dominate the current ECD spectrum. However, as for dA_6 and dC_6, a much larger variety of product ions is observed than before.

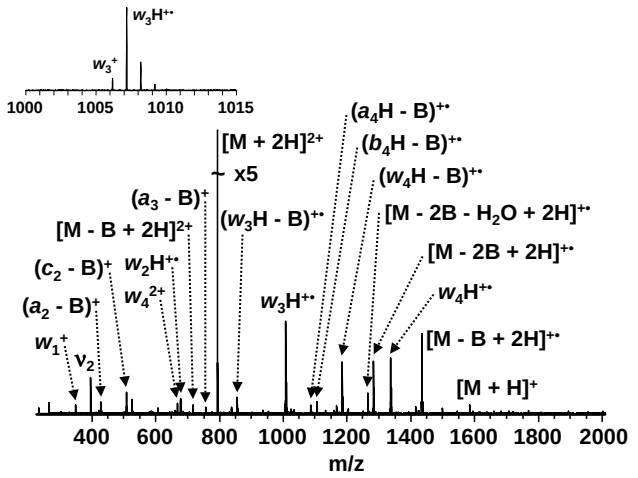

Fig. 5. ECD (20 scans) of dG_5 at the improved ECD conditions found for dA_6 and dC_6 (see Figs. 2 and 4). The spectrum differs from previous experiments in that a plentitude of product ions are observed (as for dA_6 and dC_6). However, there is also a resemblance to previous data in that several product ions are present as radical ions containing one additional hydrogen atom. In many cases, there is a mixture of even-electron and radical species, see the inset for an example. As for dA_6 and dC_6, zwitterionic precursor ions are indicated by the presence of doubly charged products. *w* ions can also be *d* ions, *b* ions can be *y* ions, *a* ions can be *z* ions, and *c* ions can be *x* ions because of the symmetrical nature of dG_5.

Table 3
Product ions observed following ECD (80 ms irradiation, −0.2 V bias, +150 V grid) of dG_5

Observed *m/z*	Calculated *m/z*	Assignment	Error (ppm)
232.08291	232.08285	$(a_1/z_1 - H_2O)^+$	0.2
348.07042	348.07038	$w_1/d_1{}^+$	0.1
428.0970	428.0971	$(a_2/z_2 - B)^+$	−0.2
508.0633	508.0630	$(c_2/x_2 - B)^+$	0.6
526.0737	526.0740	$(w_2/d_2 - B)^+$	−0.6
668.1182	668.1176	$w_4/d_4{}^{2+}$	0.9
678.1315	678.1307	$w_2H/d_2H^{+\bullet}$	1.2
686.0664	686.0670	$(c_3/x_3 - 2B)^+$	−0.8
717.1371	717.1362	$[M - B + 2H]^{2+}$	1.2
757.14964	757.14955	$(a_3/z_3 - B)^+$	0.1
792.6607	792.6607	$[M + 2H]^{2+}$	Calibrant
837.1151	837.1155	$(c_3/x_3 - B)^+$	−0.5
856.1344	856.1343	$(w_3H/d_3\ H - B)^{+\bullet}$	0.1
935.1525	935.1532	$(a_4/z_4 - 2B)^+$	−0.7
1007.184	1007.183	$w_3H/d_3H^{+\bullet}$	1.1
1025.195	1025.194	$(w_3H/d_3H + H_2O)^{+\bullet}$	1.5
1034.136	1034.138	$(w_4H/d_4H - 2B)^{+\bullet}$	−1.6
1087.209	1087.210	$(a_4H/z_4H - B)^{+\bullet}$	−1.0
1105.2214	1105.2205	$(b_4H/y_4H - B)^{+\bullet}$	0.8
1167.1756	1167.1762	$(c_4H/x_4H - B)^{+\bullet}$	−0.5
1185.186	1185.187	$(w_4H/d_4H - B)^{+\bullet}$	−0.8
1265.211	1265.213	$[M - 2B - H_2O + 2H]^{+\bullet}$	−1.6
1283.222	1283.223	$[M - 2B + 2H]^{+\bullet}$	−0.8
1336.234	1336.236	$w_4H/d_4H^{+\bullet}$	−1.5
1416.261	1416.262	$[M - B - H_2O + 2H]^{+\bullet}$	−0.7
1434.271	1434.273	$[M - B + 2H]^{+\bullet}$	−1.4
1584.3141	1584.3141	[M + H]+	Calibrant

For example, a complete *w*/*d* ion series is detected in which the four larger fragments are radical ions. Radical $(a/z - B)$, $(b/y - B)$, and $(c/x - B)$ ions are also observed. In all cases, the radical results from one additional hydrogen atom. In many cases, a mixture of the even-electron and radical species is seen, see the inset in Fig. 5 for an example. For dG_5, only one doubly charged sequence-specific product ion is detected ($w_4/d_4{}^{2+}$), indicating the presence of at least one zwitterion form.

3.5. Improved ECD of d(GCATGC)

Because thymine has a very low proton affinity [44] it was not possible to observe cations from an oligodeoxynucleotide containing thymidine residues only. Therefore, the ECD behavior of an oligonucleotide containing all four deoxynucleotides (d(GCATGC)) was investigated. The product ion spectrum following ECD is shown in Fig. 6 and assigned product ions are listed in Table 4. As for the homooligonucleotides discussed above, some major backbone fragments are the same as observed previously ($d_5{}^+$, $w_5H^{+\bullet}$, and $z_5H^{+\bullet}$). However, in addition to those product ions, an abundant w_4/d_4 ion (w_4 and d_4 have the same nucleotide composition and can, thus, not be distinguished based on mass alone) and a w_3 ion are observed along with a_4/z_4 and c_4/x_4 fragments. The product ion at *m/z* 468.06 can be assigned as either c_2 or x_2 minus a guanine base (c_2 and x_2 are isomers). However, the nucleobase closest to the cleavage site is usually lost [4], rendering $(x_2 - B)$ the most probable candidate. Product ions containing five nucleotide residues minus the base closest to the cleavage site also have possible isomers because the difference between, for example, w_5 and d_5 is cytosine versus guanine, but, that difference

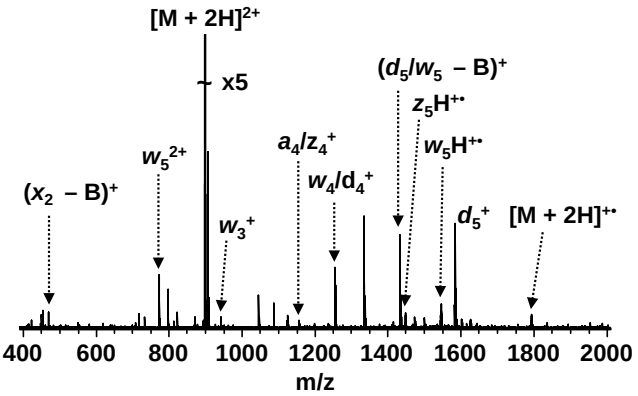

Fig. 6. ECD (20 scans) of d(GCATGC) at the improved ECD conditions found for dA_6, dC_6, and dG_5 (see Figs. 2, 4 and 5). The number of different product ions is smaller than for the three homodeoxynucleotides discussed above. However, the information content is significantly improved compared to previous experiments with the detection of two additional *w* ions (w_3 and w_4 (or d_4)), one a_4/z_4 ion, and one $(x_2 - B)$ ion. The abundance of doubly charged w_5 is higher than for the homodeoxynucleotides, which may be explained by the presence of a thymidine residue. Thymine has a much lower proton affinity than the other nucleobases and, thus, enhances the possibility of the d(GCATGC) dication to be zwitterionic.

Table 4
Product ions observed following ECD (80 ms irradiation, −0.2 V bias, +150 V grid) of d(GCATGC)

Observed *m/z*	Calculated *m/z*	Assignment	Error (ppm)
232.0825	232.0829	$(a_1 - H_2O)^+$	−1.7
468.0563	468.0573	$(c_2/x_2 - G)^+$	−2.1
707.61005	707.61009	$(x_5 - C)^{2+}/(c_5 - G)^{2+}$	−0.05
772.1370	772.1372	$w_5{}^{2+}$	−0.3
896.6801	896.6801	$[M + 2H]^{2+}$	Calibrant
941.1640	941.1629	w_3+	1.2
1156.246	1156.244	$a_4/z_4{}^+$	1.7
1236.211	1236.210	$c_4/x_4{}^+$	0.8
1254.222	1254.220	$w_4/d_4{}^+$	1.6
1334.188	1334.247	$(a_5 - G)^+/(z_5 - C)^+$??	−44
1414.217	1414.213	$(x_5 - C)^+/(c_5 - G)^+$	2.8
1432.230	1432.224	$(w_5 - C)^+/(d_5 - G)^+$	4.2
1446.301	1446.298	$z_5H^{+\bullet}$	2.1
1544.278	1544.275	$w_5H^{+\bullet}$	2.3
1583.276	1583.273	$d_5{}^+$	1.9
1642.309	1642.312	$[M - G + 2H]^{+\bullet}$	−1.8
1793.3608	1793.3608	$[M + 2H]^{+\bullet}$	Calibrant

is canceled by loss of guanine from d_5 and cytosine from w_5. Thus, those product ions could also not be uniquely assigned. Finally, an abundant $w_5{}^{2+}$ ion is observed, indicating a higher percentage of precursor ions to be zwitterions than for the homooligonucleotides discussed above. The probability of simultaneous protonation and deprotonation should increase with increasing thymine content because of its low proton affinity, consistent with the presence of one thymidine residue.

4. Conclusion

Mass-selective external ion accumulation in combination with an electron source providing a high flux of collimated electrons drastically improve the information content in ECD product ion spectra from oligodeoxynucleotides. Complete *w*/*d* ion series are observed in many cases along with several (a/z − B) and (c/x − B) ions, allowing complete oligonucleotide sequencing. However, because of the plentitude of product ions, spectral interpretation is not trivial although product ion spectra obtained from oligonucleotides with different nucleotide composition have similar appearance, contrary to previous results, rendering interpretation more straightforward. The currently observed more consistent behavior shows promise for ECD as a tool to sequence oligonucleotides. The presented ECD spectra contain evidence that populations of gas-phase oligonucleotide dications are zwitterionic. In addition, the data demonstrates potential for ECD to characterize DNA and RNA secondary structure because gas-phase intramolecular hydrogen bonding can be preserved following ECD. Future work will include an investigation of the ECD behavior of larger oligo(deoxy)nucleotides and ion-electron reactions involving nucleic acid anions, which should allow higher sensitivity.

Acknowledgements

The authors acknowledge Christopher L. Hendrickson, Alan G. Marshall, and Roman A. Zubarev for valuable discussions and suggestions. This work was supported by the University of Michigan, the National High Magnetic Field Laboratory in Tallahassee, FL, and Florida State University. Data was acquired at the NSF National High Field FT-ICR Mass Spectrometry Facility in Tallahassee, FL (CHE-99-09502).

References

[1] K.K. Murray, J. Mass Spectrom. 31 (1996) 1203.
[2] E. Nordhoff, F. Kirpekar, P. Roepstorff, Mass Spectrom. Rev. 15 (1996) 67.
[3] D.C. Muddiman, R.D. Smith, Rev. Anal. Chem. 17 (1998) 1.
[4] S.A. McLuckey, G.J. Van Berkel, G.L. Glish, J. Am. Soc. Mass Spectrom. 3 (1992) 60.
[5] S.A. McLuckey, S. Habibi-Goudarzi, J. Am. Chem. Soc. 115 (1993) 12085.
[6] Z. Wang, K.X. Wan, R. Ramanathan, J.S. Taylor, M.L. Gross, J. Am. Soc. Mass Spectrom. 9 (1998) 683.
[7] D.P. Little, R.A. Chorush, J.P. Speir, M.W. Senko, N.L. Kelleher, F.W. McLafferty, J. Am. Chem. Soc. 116 (1994) 4893.
[8] D.P. Little, F.W. McLafferty, J. Am. Chem. Soc. 117 (1995) 6783.
[9] D.P. Little, D.J. Aaserud, G.A. Valaskovic, F.W. McLafferty, J. Am. Chem. Soc. 118 (1996) 9352.
[10] J. Gross, F. Hillenkamp, K.X. Wan, M.L. Gross, J. Am. Soc. Mass Spectrom. 12 (2001) 180.
[11] J. Ni, M.M.A. Matthews, J.A. McCloskey, Rapid Commun. Mass Spectrom. 11 (1997) 535.
[12] P.P. Wang, M.G. Bartlett, L.B. Martin, Rapid Commun. Mass Spectrom. 11 (1997) 846.
[13] A.K. Vrkic, R.A.J. O'Hair, S. Foote, G.E. Reid, Int. J. Mass Spectrom. 194 (2000) 145.
[14] A. Weimann, P. Iannitti-Tito, M.M. Sheil, Int. J. Mass Spectrom. 194 (2000) 269.
[15] J. Gross, A. Leisner, F. Hillenkamp, S. Hahner, M. Karas, J. Schafer, F. Lutzenkirchen, E. Nordhoff, J. Am. Soc. Mass Spectrom. 9 (1998) 866.
[16] J.C. Hannis, D.C. Muddiman, Int. J. Mass Spectrom. 219 (2002) 139.
[17] S.A. McLuckey, J.L. Stephenson, R.A.J. O'Hair, J. Am. Soc. Mass Spectrom. 8 (1997) 148.
[18] B. Liu, P. Hvelplund, S. Brondsted Nielsen, S. Tomita, Int. J. Mass Spectrom. 230 (2003) 19.
[19] R.A. Zubarev, N.L. Kelleher, F.W. McLafferty, J. Am. Chem. Soc. 120 (1998) 3265.
[20] F.W. McLafferty, D.M. Horn, K. Breuker, Y. Ge, M.A. Lewis, B. Cerda, R.A. Zubarev, B.K. Carpenter, J. Am. Soc. Mass Spectrom. 12 (2001) 245.
[21] R.A. Zubarev, Mass Spectrom. Rev. 22 (2003) 57.
[22] B.A. Cerda, D.M. Horn, K. Breuker, F.W. McLafferty, J. Am. Chem. Soc. 124 (2002) 9287.
[23] S. Koster, M.C. Duursma, J.J. Boon, R.M.A. Heeren, S. Ingemann, R.A.T.M. van Benthem, C.G. de Koster, J. Am. Soc. Mass Spectrom. 14 (2003) 332.
[24] J.V. Olsen, K.F. Haselmann, M.L. Nielsen, B.A. Budnik, P.E. Nielsen, R.A. Zubarev, Rapid Commun. Mass Spectrom. 15 (2001) 969.
[25] A.J. Kleinnijenhuis, M.C. Duursma, E. Breukink, R.M.A. Heeren, A.J.R. Heck, Anal. Chem. 75 (2003) 3219.
[26] K. Håkansson, R.R. Hudgins, A.G. Marshall, R.A.J. O'Hair, J. Am. Soc. Mass Spectrom. 14 (2003) 23.

[27] M.E. Belov, E.N. Nikolaev, G.A. Anderson, H.R. Udseth, T.P. Conrads, T.D. Veenstra, C.D. Masselon, M.V. Gorshkov, R.D. Smith, Anal. Chem. 73 (2001) 253.
[28] C.L. Hendrickson, J.P. Quinn, M.R. Emmett, A.G. Marshall, Proceedings of 49th ASMS Conference on Mass Spectrometry and Allied Topics, Chicago, IL, 2001, CD.
[29] K.F. Haselmann, B.A. Budnik, J.V. Olsen, M.L. Nielsen, C.A. Reis, H. Clausen, A.H. Johnsen, R.A. Zubarev, Anal. Chem. 73 (2001) 2998.
[30] Y.O. Tsybin, P. Hakansson, B.A. Budnik, K.F. Haselmann, F. Kjeldsen, M. Gorshkov, R.A. Zubarev, Rapid Commun. Mass Spectrom. 15 (2001) 1849.
[31] K. Hakansson, M.J. Chalmers, J.P. Quinn, M.A. McFarland, C.L. Hendrickson, A.G. Marshall, Anal. Chem. 75 (2003) 3256.
[32] M.W. Senko, C.L. Hendrickson, L. Pasa-Tolic, J.A. Marto, F.M. White, S. Guan, A.G. Marshall, Rapid Commun. Mass Spectrom. 10 (1996) 1824.
[33] M.R. Emmett, R.M. Caprioli, J. Am. Soc. Mass Spectrom. 5 (1994) 605.
[34] B.E. Wilcox, C.L. Hendrickson, A.G. Marshall, J. Am. Soc. Mass Spectrom. 13 (2002) 1304.
[35] S.C. Beu, D.A. Laude Jr., Int. J. Mass Spectrom. Ion Processes 112 (1992) 215.
[36] A.G. Marshall, T.-C.L. Wang, T.L. Ricca, J. Am. Chem. Soc. 107 (1985) 7893.
[37] S. Guan, A.G. Marshall, Int. J. Mass Spectrom. Ion Process. 157/158 (1996) 5.
[38] E.B. Ledford Jr., D.L. Rempel, M.L. Gross, Anal. Chem. 56 (1984) 2744.
[39] S.D.-H. Shi, J.J. Drader, M.A. Freitas, C.L. Hendrickson, A.G. Marshall, Int. J. Mass Spectrom. 195/196 (2000) 591.
[40] M.W. Senko, J.D. Canterbury, S. Guan, A.G. Marshall, Rapid Commun. Mass Spectrom. 10 (1996) 1839.
[41] D.M. Horn, Y. Ge, F.W. McLafferty, Anal. Chem. 72 (2000) 4778.
[42] D.M. Horn, K. Breuker, A.J. Frank, F.W. McLafferty, J. Am. Chem. Soc. 123 (2001) 9792.
[43] K. Breuker, H. Oh, D.M. Horn, B.A. Cerda, F.W. McLafferty, J. Am. Chem. Soc. 124 (2002) 6407.
[44] K.B. Green-Church, P.A. Limbach, J. Am. Soc. Mass Spectrom. 11 (2000) 24.
[45] K.B. Green-Church, P.A. Limbach, M.A. Freitas, A.G. Marshall, J. Am. Soc. Mass Spectrom. 12 (2001) 268.
[46] M.J. Chalmers, K. Hakansson, R. Johnson, R. Smith, J. Shen, M.R. Emmett, A.G. Marshall, Proteomics (2004) 970.
[47] A.G. Marshall, S. Guan, Rapid Commun. Mass Spectrom. 10 (1996) 1819.
[48] M.L. Nielsen, B.A. Budnik, K.F. Haselmann, J.V. Olsen, R.A. Zubarev, Chem. Phys. Lett. 330 (2000) 558.
[49] R.A. Zubarev, Personal communication.